BAUET JOURNAL
Published by
Bangladesh Army University of Engineering & Technology (BAUET)
Journal Homepage: https://journal.bauet.ac.bd/
DOI: https://doi.org/10.59321/BAUETJ.V5I1.1

Static Analysis Based Bus Ranking in Power Systems Using PV/QV Curves to Improve Voltage Stability and Reactive Power Margin

Md. Saiful Islam[1,2*], Md. Rubel Basar[1], Md. Abdullah Al-Moti Pinto[1], Md. Towhidul Islam[2]

[1]*Department of Electrical and Electronic Engineering, Bangladesh Army University of Engineering & Technology, Qadirabad, Natore-6431, Bangladesh*
[2]*Department of Electrical and Electronic Engineering, Bangladesh University of Engineering and Technology, Dhaka 1205, Bangladesh*

Abstract: Voltage stability is a critical concern in modern power systems, particularly for ensuring a safe and reliable operation under heavily loaded conditions. This study presents a static voltage stability assessment (VSA) approach applied to the IEEE 14-bus test system, focusing on the identification and ranking of load buses using PV and QV curve analysis to guide optimal reactive power compensation. Simulation results identify Bus 14 as the most vulnerable, with the lowest real power margin (153.35 MW) and reactive power margin (-117.01 MVAR). To mitigate voltage instability, Static VAR Compensators (SVCs) and Static Capacitor (SC) banks were strategically deployed at this critical bus. Post-compensation analysis reveals a significant enhancement in voltage stability: the critical voltage at Bus 14 improved from 0.5936 pu to 0.9183 pu (a 54.7% increase), and the real power margin increased from 135.35 MW to 224.99 MW. Similarly, the minimum reactive power margin improved from -117.14 MVAR to -220.52 MVAR, while the corresponding critical voltage rose from 0.54 pu to 0.94 pu. These shifts in both PV and QV curves indicate enhanced reactive power support and a stronger voltage profile.

Keywords: *Bus Ranking; IEEE 14 Bus System; PV/QV Curve; Voltage Stability; Reactive Power Margin; Static Var Compensator*

Introduction: Maintaining voltage stability is crucial for operating modern power systems. It guarantees that reasonable voltage levels which is 95% to 105% of the rated value is maintained at all buses under various load and disturbance conditions [1]. Voltage instability is becoming more common due to the stress on aging infrastructure, the increase in nonlinear loads, and the integration of intermittent renewable sources. Poor bus voltage control or insufficient reactive power support can cause progressive voltage drops, so causing system collapse and blackouts. Maintaining safe and stable power system operation depends thus on buses having enough reactive power margin [2].

Researchers have developed a variety of analytical tools and indices to assess the susceptibility to voltage collapse of power system. Among them, PV and QV curves are widely recognized because of their simplicity and effectiveness in static analysis. These curves give insight about voltage behavior under incremental loading and help to estimate maximum reactive power requirement and loading limit of individual buses. Many Voltage Stability Indices (VSIs) and power flow equations have also been extensively discussed [3]. Rao et al. focused the use of these indices in load ability analysis, weak bus identification, and voltage collapse

estimation [4]. Mokred et al. suggested the Modern Stability Assessment Index (MSAI) to increase the precision of identifying stressed areas in power systems [5], while Yadav et al. offered a qualitative framework for selecting VSIs tailored to specific system characteristics [6]. Recent studies have further developed these

concepts. Hemmatpour developed a method to determine Voltage Stability Indices (VSIs) at buses without direct measurements through predictive models [7], whereas Alayande et al. utilized L-Index values to identify vulnerable buses and enhance voltage profiles through reactive power support [8]. Hao et al. created a short-term voltage solvability indicator by eigenvalue analysis of the reduced Jacobian matrix [9]. Gadal et al. conducted a comparative study integrating VSIs with FACTS devices for reactive power compensation [10]. Nitsch et al. examined uncertainty modeling in dynamic simulations to assess stability margins amid model variances [11]. Rezaee et al. emphasized the importance of proper coordination of under-frequency and under-voltage load shedding method to maintain stable voltage and frequency [12].

Several comparison analyses and simulation-based investigations have further evaluated the advantages and disadvantages of current VSI methodologies. Salama et al. discussed the computational complexity and performance of 49 VSIs across several power system models [3]. Werkie et al. presented a state-of-the-art review on voltage control strategies and classified reactive power enhancement techniques [13]. Gupta et al. considered voltage stability assessment under integrated wind and solar PV scenarios [14], whereas Ehimhen et al. employed predictive optimization for instability identification inside the Nigerian transmission network [15]. Alabbas et al. focused a data-driven method for the prediction of real-time voltage stability status

Article history:
Received 17 June 2025
Received in revised form: 27 August 2025
Accepted 21 September 2025
Available online 15 December 2025

Corresponding author details: Md. Saiful Islam
E-mail address: saifulislambuet17@gmail.com
Tel: +8801879228632

using artificial intelligence method [16]. Ahmadipour et al. proposed a deep learning-fused gravitational search and particle swarm optimization hybrid model for an improved control [17]. Despite the extensive studies conducted, several challenges still exist. Many approaches depend solely on singular indices or exclusively on either PV or QV curve analysis. Only a limited number of researches incorporate both PV and QV attributes to establish a comprehensive and measurable ranking of buses. Furthermore, while several papers propose reactive power improvement using FACTS devices [18] or static compensators [19], they often do so without a curve-based vulnerability assessment. Even hybrid VSI methods using optimization techniques [20] or deep learning [21] fail to tie simulation data back to real-world reactive margin deficiencies. Nonetheless, there exists gaps in combining curve-based weak bus identification with practical mitigation measures. This paper introduces a unique methodology that employs both PV and QV curve studies to evaluate the buses of the IEEE 14-bus system for voltage stability.

Overview of Power System Stability: Power system stability means the ability of the system to restore operational balance after a disturbance, keeping the key variables within acceptable limit to preserve integrity of the system [22]. Disturbances may include faults, load/generation changes, or switching actions. Classifying stability into distinct categories aids to identify causes of instability and develop effective mitigation strategies. Fig. 1 illustrates the overall structure of power system stability where the voltage stability is a concerning issue with the ability of a power system to keep voltages within an acceptable range, both during normal operation and following any disturbances [23]. Voltage instability occurs when disturbances or load increases cause a sustained amount of voltage drop. It is classified as large-disturbance (response to major faults or outages) and small-disturbance (response to minor load changes) voltage stability. Further, voltage stability can be short-term or long-term, as shown in Fig. 1. Short-term stability relies on quick-acting elements like induction motors and HVDC converters, in contrast, long-term stability is influenced by slower devices, including tap-changing transformers and generator limiters.

Static Voltage Stability Assessment: Voltage Stability Indices provide a way to evaluate the voltage stability of a power system [3]. There are a number of indices that can be used to rank the stability of individual line connecting two buses in a network, or evaluate the voltage stability margins of the buses of an interconnected system based on different parameters. In this analysis two indices including i) PV curve and ii) reactive power margin is used to evaluate bus voltage stability.

PV Curve: The PV analysis is a method used to understand voltage variations with active power change. PV curve analysis is utilized to assess voltage stability in both radial systems and extensive meshed networks [24].

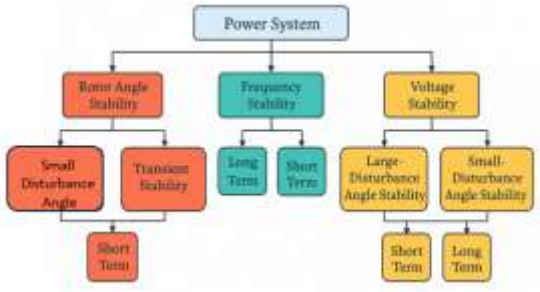

Fig. 1: Comprehensive classification of power system stability [22].

To explain PV curve analysis, let us consider a simplified network of two-bus system with a single generator, a single transmission line and a single load, as shown in Fig. 2. Here, V_1 is the transmitting end voltage and V_2 is receiving end voltage. The receiving end voltage, V_2 can be calculated as

$$|V_2|^2 = \frac{1 - \beta P_D \pm \sqrt{1 - P_D(P_D + 2\beta)}}{2} \quad \text{eq. 1}$$

where, β is constant and P_D is real-power at load.

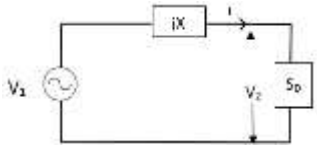

Fig. 2: Simplified two-bus power system model.

The voltage at the load point is affected by the power supplied to the load, reactance of the line and the power factor of load as indicated in the eqn. (1). The voltage stability margin in PV curve is illustrated in Fig. 3. As it can be seen from this figure, there is a critical limit $C_{critical}$, above which all the solutions deliver a stable value. The point where the two voltage solutions converge into a single value, that indicates the steady state voltage collapse point. The load carrying capability is kept such that the voltage of a certain bus must fall in the range between $0.95\ pu$ to $1.05\ pu$ of the rated value of the voltage. At the knee of the

PV curve, the voltage drops quickly as the load rises. PV curves are effective for voltage stability assessment specially for radial systems.

Reactive Power Margin: Reactive power margin quantifies the system's ability to supply additional reactive power demand without violating voltage limits or triggering voltage collapse. Reactive power margin is typically evaluated through QV curve analysis. This margin is thus directly linked to load-bearing limit of a certain bus and serves as a preventive metric that operators can use it to identify weak areas in the system and implement remedial actions to enhance voltage support.

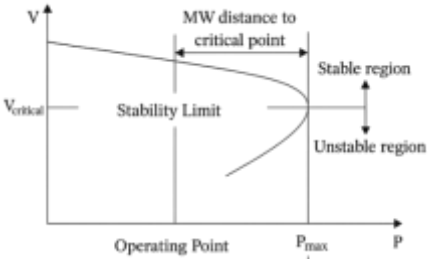

Fig. 3: PV curve illustrating voltage stability margin [25].

The QV curve is drawn for a specific load bus, and this plot is basically a curve of reactive power injection versus the resulting bus voltage. The eqn. (2) shows that there are two possible solutions. The rightward solution is in the stable operating region, and the leftward solution is in the unstable region. The difference between the current operating point and this critical point defines the reactive power margin as shown in Fig. 4.

$$Q_D = -|V_2|^2 B + |V_1||V_2| B \cos(\theta_{12}) \quad \text{eq. 2}$$

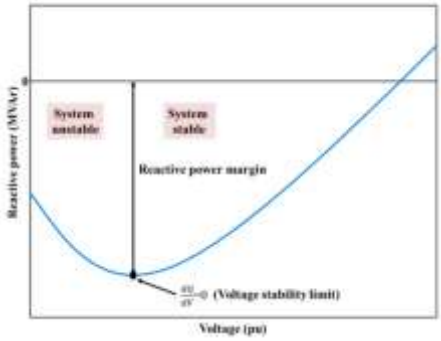

Fig. 4: QV curve showing voltage stability limit and reactive power margin [26].

Voltage Stability Improvement: Voltage stability improvement refers to the set of strategies or actions that is undertaken to enhance a power system's ability to maintain acceptable voltage levels, both during normal operating condition and in the event of disturbances. Enhancing voltage stability is crucial for a secure and reliable functioning of power systems. There are a number of devices that is currently used to stabilize voltage profile in the buses of an interconnected system [27].

Static Var Compensator: Static Var Compensator (SVC) is a power electronics-based device that connects in parallel with the power system for voltage stability improvement. It can provide dynamic stability improvement by means of a controller. It is a combination of Thyristor Switched Capacitors (TSC) and Thyristor Controlled Reactors (TCR) connected in parallel. SVC also integrates filters and a control system to ensure its effective and reliable operation.

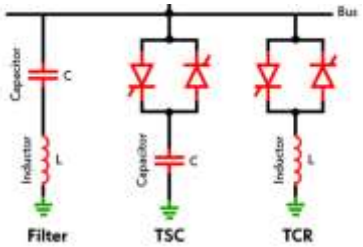

Fig. 5: Construction of SVC [28].

The TSC is used to manage the capacitive reactive power, while the TCR is responsible for controlling the inductive reactive power. This dual capability allows the SVC to precisely regulate reactive power flow. If the voltage level in the system rises above the desired threshold, the SVC will promptly absorb reactive power to restore it. Conversely, if the voltage level drops below the desired threshold, the SVC will inject reactive power into the system. to bring it back. The SVC's control system achieves this by adjusting the "firing angle" of the thyristor devices. This adjustment regulates the amount of reactive power that is injected or absorbed by the TCR and TSC. This dynamic and accurate control allows the SVC to maintain a stable voltage level and improve the overall power factor of the system.

Static Capacitor Bank: Static capacitor bank improves voltage stability by injecting reactive power, compensating for voltage drops, and enhancing the overall voltage profile [29]. It is static in nature unlike SVC as there is no control mechanism to control how much capacitance is needed to improve voltage stability in certain case but it is very cheap. So, in most cases the amount needs to be handled manually. The amount of capacitance needed can be found from the eqn. (4). Capacitor bank can be used both in wye and del configurations as shown in Fig. 6. The value of the capacitor can be calculated as:

$$C = \frac{Q_c}{\omega V_{Rms}^2} \qquad \text{eq. 3}$$

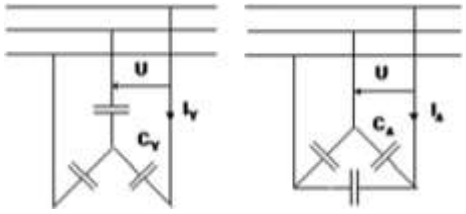

Fig. 6: Different configuration of capacitor bank with 3 phase lines [30].

System Modelling: IEEE-14 bus system is chosen as the test network. The single-line diagram (SLD) of the system is presented in Fig. 7. The IEEE 14 Bus test system is a basic approximation of the American power grid, it is a simplified representation of the transmission system in the Midwest of United States [31]. As its name suggests, the system comprises 14 different buses along with 11 loads, 5 generators, 5 transformers and 16 transmission lines. The system operates at a nominal frequency of 50 Hz. All network parameters provided in per unit values based on 100 MVA base.

The synchronous generators are connected in bus 1, 2, 3, 6 and 8. Among these, bus 1 is considered as the slack bus, therefore the voltage magnitude and voltage angle are given for this bus. The remaining generators are set up to regulate active power injection and voltage levels at the associated buses. Bus voltages are maintained at different level at each bus. Total Installed Capacity is 700 MW and the spinning reserve is 130.59MW. The length of each line in the Power Factory model is set to 1km. The loads are modeled as having constant active and reactive power demand. Each transformer's rated power is taken to be 100 MVA.

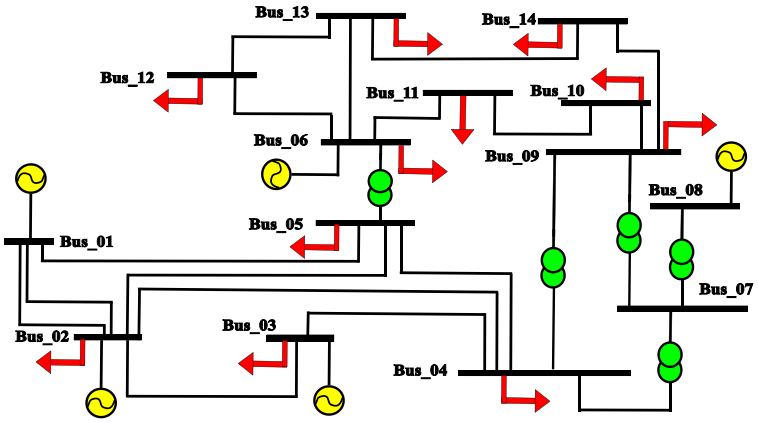

Fig. 7: Single line diagram of the IEEE 14-bus test system.

Optimization Problem Formulation and Proposed Methodology: This section includes the systematic approach of formulating the optimization problem along with a detailed description of the proposed methodology at the end.

Optimization Approach: The optimal placement of the reactive power compensator is determined by directly at the common weakest bus while their sizing is determined by two objective functions. The primary objective is to maximize the minimum reactive power margin of the all-load buses and minimize the total installed reactive power compensation capacity while satisfying voltage stability criteria so that investment cost can be reduced. This ensures even the most vulnerable bus will achieve a strong margin. This can be expressed in mathematically by:

$$Maximize(Q_{margin,total}) = \Sigma_{i \in Load\ Buses}(Q_{margin,i}) \quad \text{eq. 4}$$

Where Q_{margin} is the reactive power margin of i^{th} bus before compensation.

$$Minimize\left(Q_{comp,total}\right) = \Sigma_{j \epsilon Compensator\ Locations}(Q_{SVC,j} + Q_{cap,j}) \quad \text{eq. 5}$$

Where $Q_{SVC,j}$ and $Q_{cap,j}$ are the reactive power capacity of SVC and SC respectively installed at the bus j. Now some constraints will be discussed that will control the objective function.

- **Voltage Limit:** All bus voltage must remain within the acceptable voltage range under all operating conditions and after compensation, according to $V_{min} < V_k < V_{max}$.
- **Compensator Capacity Limits:** Installed compensator size must be within their practical operating ranges like $0 < Q_{SVC,j} < Q_{SVC,max}$ and $0 < Q_{cap,j} < Q_{cap,max}$.
- **Power Flow Equation:** Power system operation must always obey the power flow equation.

$$\begin{aligned} P_{G_k} - P_{L_k} &= \sum_{m=1}^{N} |V_k||V_m||Y_{km}| \cos(\delta_k - \delta_m - \theta_{km}) \\ Q_{G_k} - Q_{L_k} &= \sum_{m=1}^{N} |V_k||V_m||Y_{km}| \sin(\delta_k - \delta_m - \theta_{km}) \end{aligned} \quad \text{eq. 6}$$

Where, $P_{G_k}, Q_{G_k}, P_{L_k}, Q_{L_k}, V_k, Y_{km}, \theta_{km}$ are active power generation, reactive power generation, active loads, reactive loads, voltage magnitude, voltage angle and admittance matrix elements respectively.

Stepwise Description of the Proposed Methodology: This section presents systematic overview of the entire procedure from the identification of the weakest buses in a power system network to the implementation of improvement technique as visually demonstrated in the flowchart depicted in Fig. 8. The first step involves establishing the foundation of the power system model to be analyzed which is IEEE-14 bus system in this case. For each i^{th} load bus, PV/QV curves are generated by continuously increasing active and reactive power, respectively. From these curves, voltage magnitude and real power margin are recorded at the "knee point" of PV curve. Reactive power margin and corresponding voltage magnitude are also recorded from the QV curve. Following this, comprehensive ranking is performed independently based on the real power margin and reactive power margin for each load bus. The common weakest bus is identified from the two ranking then reactive power compensator like SVCs, SC are designed and sized according to the objective function. After successfully implementation of reactive power compensator, new PV and QV curve are generated and compared with the pre-compensation curve to validate the effectiveness.

Results and Analysis: The simulation results based on our static analysis using PV/QV curve are presented in this section. All the simulation results presented in this section have been obtained by using a comprehensive power system analysis software DIgSILENT Power-Factory which is used widely in academia and industry. Fig. 9 illustrates two key aspects: (a) the PV curves of various load buses and (b) the ranking of buses based on their real power margins in the IEEE 14-bus test system. For each bus, the active power demand was gradually increased, and the corresponding bus voltage was recorded. The voltage characteristics of each load bus under varying load conditions are depicted in Fig. 9 (a). A critical point on this curve, known as the "knee point" or critical voltage is identified that signifies the maximum active power that a bus can handle before its voltage rapidly collapses. To further clarify this, the real power margin of individual buses is ranked in Fig. 9 (b).

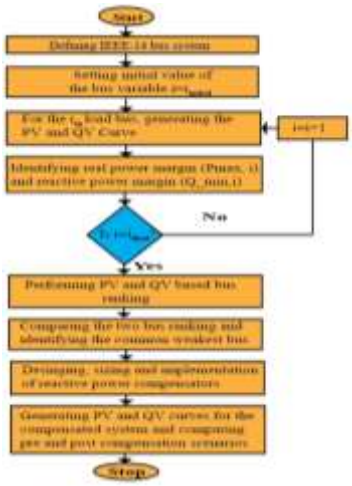

Fig. 8: Step by step illustration of the proposed methodology.

Where it can be seen that the bus 14 exhibits the lowest real power margin which is 153.3486 MW followed by bus 10, bus 12, bus 11, bus 7, bus 9, bus 13, bus 5 and bus 4. So, bus 14 is the weakest location in this network. Based on this analysis, bus 14, bus 10, bus 12, and bus 11 can be identified as weak bus, indicating a high risk of voltage instability. Bus 7, bus 9 and bus 13 are classified as moderately weak, while bus 5 and bus 4 are considered strong buses, having relatively higher stability limit.

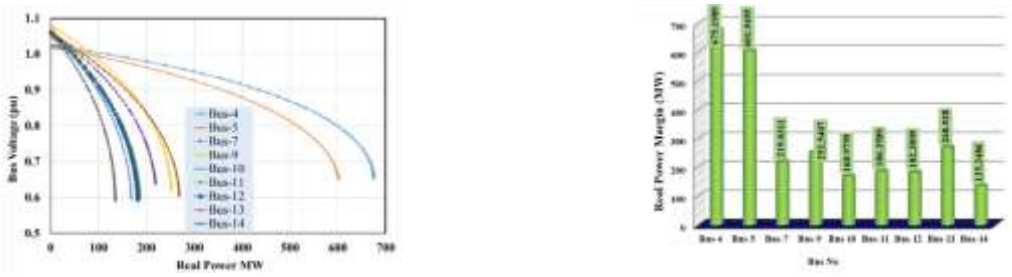

(a) (b)

Fig. 9: (a) PV Curve and (b) Ranking of load Buses for IEEE 14 Bus System.

Bus 4 can be identified as the strongest location in this network as it exhibits highest real power margin which is 675.1989 MW. It represents the availability of reactive power reserve of a bus can provide or absorb before reaching its voltage stability limit. A smaller reactive power margin indicates higher vulnerability on the other hand higher reactive power margin indicates higher stability. The Fig. 10 (b) illustrates a ranking of the reactive power margins from the simulated QV curves for each bus. As it can be seen from Fig.10(b), bus 14 consistently demonstrates the lowest reactive power margin which is -117.0147 MVAR followed by bus 12, bus 10, bus 11, bus 9, bus 13, bus 7, bus 5 and bus 4. So, again it can be decided that bus 14 is the weakest location in this network. According to the analysis we can say that bus 14, bus 12, bus 10, bus 11 are weak bus. Bus 9, bus 13 and bus 7 are moderately weak. Bus 5 and bus 4 are strong buses. Similar to the PV curve analysis bus 4 can be seen as the strongest location in this network based on the QV curve analysis.

(a) (b)

Fig. 10: (a) QV Curve and (b) Ranking of load Buses for IEEE 14 Bus System.

A comparative analysis of the bus ranking is derived independently from both PV and QV curve though Fig. 9(b) and Fig. 10(b) reveals that bus ranking is not totally identical across the two assessment approaches. For example, the PV curve-based ranking identifies bus 10 as the second weakest and bus 12 as the third weakest. Conversely, the QV curve-based ranking places bus 12 as the second weakest and bus 10 as the third weakest. Another dissimilarity is found for bus 7, bus 9 and bus 13. According to PV curve-based ranking among this three buses bus 7 is the weakest and bus 9 is weaker than bus 13, on the other hand as per the QV curve based ranking bus 9 is the weakest among this three and bus 13 is weaker than bus 7. This distinction arises because PV and QV analyses considers different factors of voltage stability. The PV method analyses system stability based on active power loading on the other hand QV method assesses reactive power capacity and margin for system voltage stability. So, it is possible for a bus to exhibit robust active power transfer capabilities yet provides a limited reactive power margin or vice versa. But in our simulation bus 14 come consistently as the weakest bus as it shows lowest real power margin as well as lowest reactive power margin. That's why this location is considered the weakest position in this IEEE 14 network system. Table.1 summarizes the simulation result with stable operating limit.

Voltage Stability Improvement of Bus 14: In this section reactive power compensation was successfully implemented to mitigate voltage stability challenge at bus 14 as this location is identified the weakest position in the network. For sizing and modeling of SVC and SC-QV characteristics of that bus and objective function is considered. The goal was to maximize the voltage stability of the weakest bus by ensuring its voltage magnitude was raised to an acceptable level, while simultaneously maximizing the overall reactive power margin of the entire system and minimizing the size of compensation devices like SVCs and SCs.

Table.1. Operating Characteristics of Bus from PV/QV Curve

From PV Curve			Form QV Curve			Comments
Bus Ranking	P Limit (MW)	P Margin (MW)	Bus Ranking	Q Limit (MVAR)	Q Margin (MVAR)	
Bus-14	56.4144	135.3486	Bus-14	-40.8985 to 12.3332	-117.0147	Weakest
Bus-10	67.2543	168.9759	Bus-12	-73.1320 to 3.57810	-175.4108	Weak
Bus-12	50.5800	182.3009	Bus-10	-69.8801 to 7.05960	-180.1464	Weak
Bus-11	74.8965	186.3589	Bus-11	-79.5453 to 2.71710	-195.5435	Weak
Bus-7	98.4039	219.0311	Bus-9	-95.1026 to 4.70490	-237.3807	Moderate
Bus-9	123.779	252.5407	Bus-13	-112.600 to 11.4194	-283.0113	Moderate
Bus-13	111.9393	268.9280	Bus-7	-137.265 to -0.6783	-337.5137	Moderate
Bus-5	224.8924	601.9495	Bus-5	-174.345 to 105.323	-593.1558	Strong
Bus-4	298.4584	675.1989	Bus-4	-171.56 to 115.0179	-601.0912	Strongest

The optimization was constrained by a stable operating voltage, practical compensator sizes, and adherence to power balancing equations. The efficacy of this compensation then validated by comparing the PV and QV curve before and after compensation state. The improved PV and QV curves for Bus 14 are presented in Fig. 11(a) and 11(b).

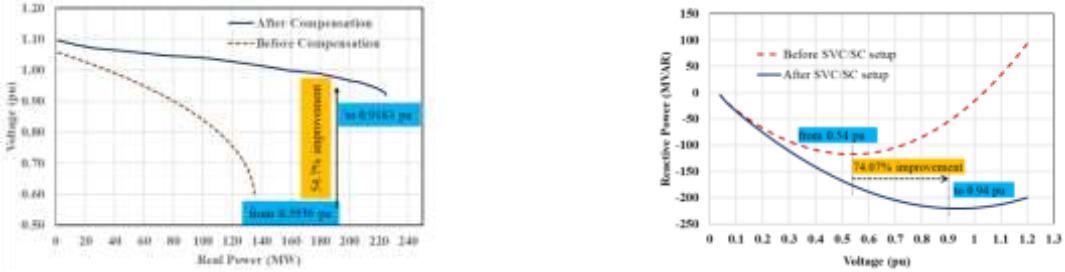

(a) (b)

Fig. 11: (a) Improved PV and (b) QV Curve of Bus 14 for IEEE 14 Bus System.

The PV curve in Fig. 11(a) graphically depicts the voltage stability improvement as the curve is distinctly shifted to the upward and rightward direction. Now the bus can supply much more real power while maintaining its stable operating condition than before. This shift demonstrates clearly evidence of a substantial improvement in the bus's voltage stability. The critical voltage for bus 14 was recorded at $0.5936\,pu$, corresponding to active power transfer of 135.3486 MW. After implementation of

compensation the critical value of voltage remarkable increase to $0.9183\,pu$ which is nearly within the stable operation condition, corresponding to 224.987 MW active power transfer. This significant improvement nearly 54.7% in critical voltage and real power margin shows that Bus 14 is now capable of sustaining much more stable voltage level even when active power loading is increased to this bus than before.

The QV curve in Fig. 11(b) depicts improvement of reactive power margin as the curve distinctly shifted to the downward and rightward direction. Before compensation, bus 14 exhibited minimum reactive power requirement of $-117.147\,MVAR$ at a critical voltage of $0.54\,pu$, while after efficient deployment of SVC and SC the Qmin improved to $-220.5165\,MVAR$ at the critical voltage of $0.94\,pu$. Critical value of the voltage is significantly elevated from $0.54\,pu$ to $0.94\,pu$ which is nearly stable operating condition along with the reactive power margin. The shift to a higher operating voltage at the minimum Q point indicates that the system is operating further from the voltage collapse point. This signifies that the bus can now maintain more stable voltage profile even under substantial reactive power demand.

Conclusion: The PV and QV curve-based static analysis approach to assess and enhance voltage stability in the IEEE 14-bus system is presented in this paper. Compared to dynamic simulations, the PV/QV method offers a faster, computationally efficient, and visually intuitive means of identifying voltage instability and evaluating reactive power margins. As the analytical results indicated, bus 14 was identified as the weakest node, exhibiting the lowest real and reactive power margins. Reactive power support was then applied at this bus using Static VAR Compensators (SVCs) and Static Capacitor (SC) banks, resulting in a marked improvement in voltage stability is confirmed by significant shifts in the PV and QV curves. The proposed method not only proves effective for the test system but also lays the groundwork for future research on larger networks (such as IEEE 30, 57, and 118 bus systems), real-time PMU-based monitoring, and the integration of advanced control and optimization techniques like metaheuristics and adaptive control, offering a robust and scalable solution for voltage stability enhancement in smart grid environments.

References:

[1] N. M. Saman et al.,Optimization Techniques to Minimize the Power Loss and Maintain Voltage Stability for A Power System, in 2024 IEEE International Conference on Advanced Power Engineering and Energy (APEE), Sep. 2024, p. 117–122.
[2] C. W. Taylor, Power System Voltage Stability, McGraw-Hill, New York, 1994. Scientific Research Publishing." Accessed: Aug. 25, 2025. [Online]. Available: https://www.scirp.org/reference /referencespapers?referenceid=636643.
[3] H. S. Salama and I. Vokony, Voltage stability indices–A comparison and a review, Comput. Electr. Eng., vol. 98, p. 107743, Mar. 2022.
[4] A. Nageswa Rao, P. Vijaya, and M. Kowsalya, Voltage stability indices for stability assessment: a review, Int. J. Ambient Energy, vol. 42, no. 7, p. 829–845, May 2021
[5] S. Mokred and Y. Wang, Voltage stability assessment and contingency ranking in power systems based on modern stability assessment index, Results Eng., vol. 23, p. 102548, Sep. 2024.
[6] L. K. Yadav et al., "A Framework for Qualitative Analysis of Voltage Stability Indices (VSIs)," IEEE Access, vol. 12, p. 124231–124259, 2024.
[7] M. H. Hemmatpour, Prediction of voltage stability index in buses without measurement in distribution systems, IET Gener. Transm. Distrib., vol. 18, no. 14, p. 2435–2451, 2024.
[8] A. S. Alayande, A. O. Hassan, F. Olobaniyi, S. O. Osokoya, A. I. Adebeshin, and A. B. Ogundare, L-Index-Based Technique for Voltage Collapse Prediction and Voltage Stability Enhancement in Electrical Power Systems, ABUAD J. Eng. Res. Dev. AJERD, vol. 7, no. 1, p. 260–277, Jun 2024.
[9] W. Hao, X. Wang, Y. Yao, D. Gan, and M. Chen, Short-term voltage stability analysis in power systems: A voltage solvability indicator, Int. J. Electr. Power Energy Syst., vol. 161, p. 110185, Oct. 2024.
[10] R. Gadal, A. Oukennou, F. El Mariami, A. Belfqih, and N. Agouzoul, Voltage Stability Assessment and Control Using Indices and FACTS: A Comparative Review, J. Electr. Comput. Eng., vol. 2023, no. 1, p. 5419372, 2023.
[11] D. Nitsch and H. Vennegeerts, Evaluation of Simulations for Short-Term Voltage Stability Assessment with Respect to Model Uncertainties, Eng, vol. 6, no. 3, p. 41, Mar. 2025.
[12] M. Rezaee, S. Mortazavi, and A. Saffarian, Combination UFLS and UVLS Aim to Restore Frequency and Voltage Stability Simultaneously, in 2025 Fifth National and the First International Conference on Applied Research in Electrical Engineering (AREE), Feb. 2025, p. 1–7.
[13] Y. G. Werkie, G. N. Nyakoe, and C. W. Wekesa, Power System Voltage Stability Assessment and Control Strategies: State-of-the-Art Review, J. Electr. Comput. Eng., vol. 2025, no. 1, p. 6667482, 2025.
[14] S. K. Gupta and S. K. Mallik, Voltage Stability Assessment of Power System Using Line Indices with Wind System and Solar Photovoltaic Generation Integration, J. Oper. Autom. Power Eng., vol. 13, no. 4, pp. 303–314, Dec. 2025.
[15] E. A. Ehimhen, C. O. Ahiakwo, S. L. Braide, and H. N. Amadi, Voltage Instability Prediction of Nigerian 330kv Network Using Arithmetic Moving Average and Predictive Optimizer Technique.
[16] F. Kh. Alabbas, M. Khalilifar, S. M. Shahrtash, and D. A. Khaburi, A Novel Data Driven Model for Voltage Stability Status Prediction and Instability Mitigation, Int. Trans. Electr. Energy Syst., vol. 2025, no. 1, p. 6575682, 2025.
[17] M. Ahmadipour, Z. Ali, and H. M. Ridha, Enhancing voltage stability and load shedding optimization through a fusion of gravitational search algorithm and particle swarm optimization with deep learning, Soft Comput., vol. 29, no. 2, p. 701–721, Jan. 2025.
[18] Y.-W. Liu, S.-H. Rau, C.-J. Wu, and W.-J. Lee, Improvement of Power Quality by Using Advanced Reactive Power Compensation, IEEE Trans. Ind. Appl., vol. 54, no. 1, pp. 18–24, Jan. 2018.
[19] S. Sharma et al., A Comprehensive Review on STATCOM: Paradigm of Modeling, Control, Stability, Optimal Location, Integration, Application, and Installation, IEEE Access, vol. 12, p. 2701–2729, 2024.
[20] S. Mokred, Y. Wang, and T. Chen, Modern voltage stability index for prediction of voltage collapse and estimation of maximum load-ability for weak buses and critical lines identification, Int. J. Electr. Power Energy Syst., vol. 145, p. 108596, Feb. 2023.

[21] M. Zhang, J. Li, Y. Li, and R. Xu, Deep Learning for Short-Term Voltage Stability Assessment of Power Systems, IEEE Access, vol. 9, p. 29711–29718, 2021.
[22] P. Kundur et al., Definition and classification of power system stability IEEE/CIGRE joint task force on stability terms and definitions, IEEE Trans. Power Syst., vol. 19, no. 3, p. 1387–1401, Aug. 2004.
[23] T. Cutsem and C. Vournas, Voltage Stability of Electric Power Systems. Boston, MA: Springer US, 1998.
[24] Voltage Stability - an overview ScienceDirect Topics." Accessed: Aug. 25, 2025. [Online]. Available: https://www.sciencedirect.com/topics/engineering/voltage-stability
[25] Voltage sensitivity-based site selection for PHEV charging station in commercial distribution system | IEEE Conference Publication, IEEE Xplore. Accessed: Aug. 25, 2025. [Online]. Available: https://ieeexplore.ieee.org/abstract/document/6837191
[26] T. Aziz, N.-A. Masood, S. R. Deeba, W. Tushar, and C. Yuen, A methodology to prevent cascading contingencies using BESS in a renewable integrated microgrid, Int. J. Electr. Power Energy Syst., vol. 110, p. 737–746, Sep. 2019.
[27] B. Ismail, N. I. Abdul Wahab, M. L. Othman, M. A. M. Radzi, K. Naidu Vijyakumar, and M. N. Mat Naain, A Comprehensive Review on Optimal Location and Sizing of Reactive Power Compensation Using Hybrid-Based Approaches for Power Loss Reduction, Voltage Stability Improvement, Voltage Profile Enhancement and Loadability Enhancement, IEEE Access, vol. 8, p. 222733–222765, 2020.
[28] E. Technology, What is Static VAR Compensator - SVC? Power Factor Correction, ELECTRICALTECHNOLOGY. Accessed: Aug. 25, 2025. [Online]. Available: https://www.electricaltechnology.org/2023/02/static-var-compensator-svc.html
[29] A. A. Eladl, M. I. Basha, and A. A. ElDesouky, Multi-objective-based reactive power planning and voltage stability enhancement using FACTS and capacitor banks, Electr. Eng., vol. 104, no. 5, p. 3173–3196, Oct. 2022.
[30] M. Iorgulescu and D. Ursu, Reactive Power Control and Voltage Stability in Power Systems, in Reactive Power Control in AC Power Systems: Fundamentals and Current Issues, N. Mahdavi Tabatabaei, A. Jafari Aghbolaghi, N. Bizon, and F. Blaabjerg, Eds., Cham: Springer International Publishing, 2017, p. 227–248.
[31] L. L. Freris and A. M. Sasson, Investigation of the load-flow problem, Proc. Inst. Electr. Eng., vol. 115, no. 10, p. 1459–1470, Oct. 1968.